Instrumental Characterization of SCExAO VAMPIRES

Manxuan (Rebecca) Zhang, Maxwell Millar-Blanchaer, Boris Safonov,
Miles Lucas, Lucinda Lilley, Jaren Ashcraft, Barnaby Norris, Julien Lozi,
Olivier Guyon, Michael Bottom

Polarization of Circumstellar Disks

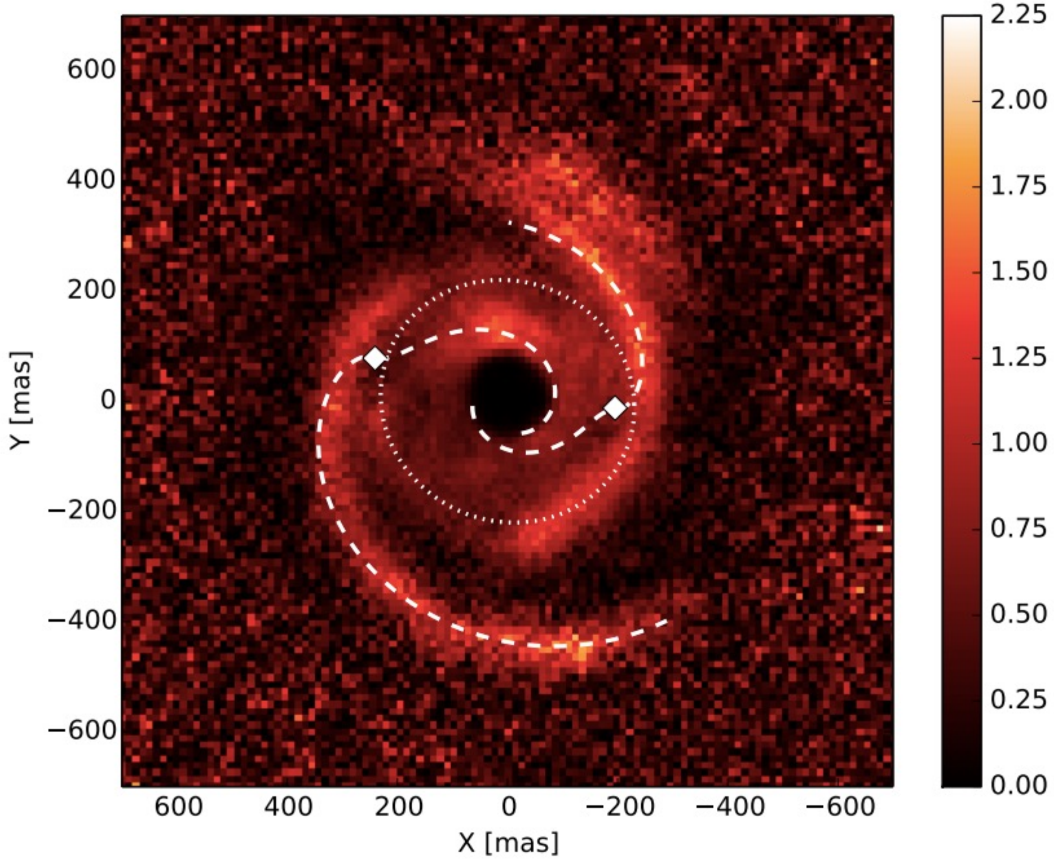

Polarized intensity showing spiral arms of MWC 758 with SPHERE (Benisty 2014)

Advantages of Polarimetric Imaging

- Detecting fainter disks at smaller separations (~0.1“)
- Well-suited to disks that appear face-on
- Characterization of scattering particles

CQ Tau Disk

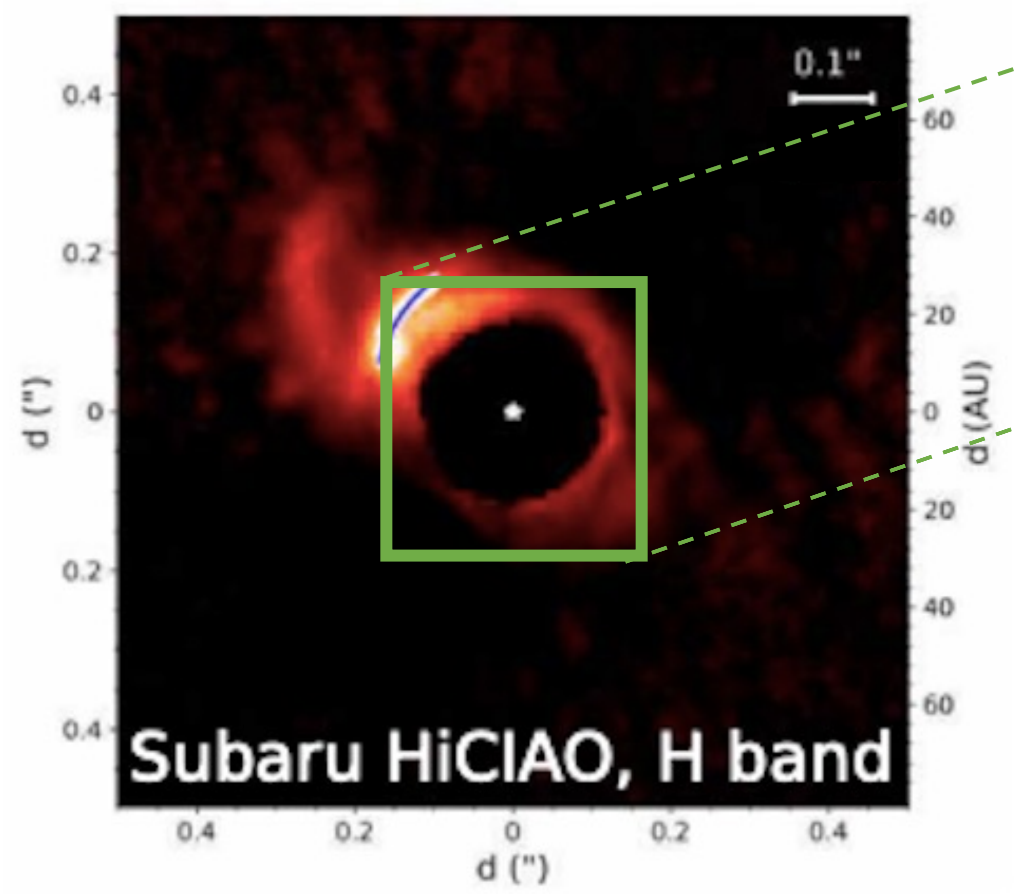

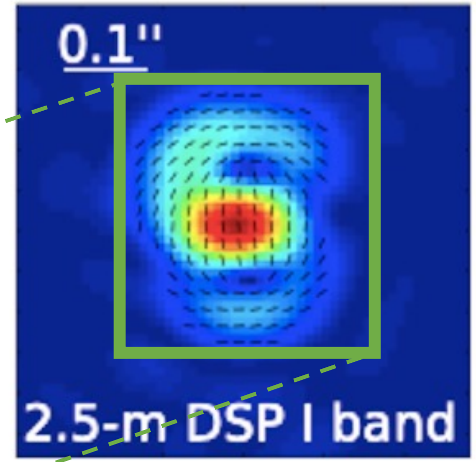

Left: Subaru/HiCIAO H band image of spiral on an 8.2m telescope (Uyama 2019)

Right: Polarized intensity in I band on a 2.5m telescope (Safonov 2019)

Polarimetry Basics

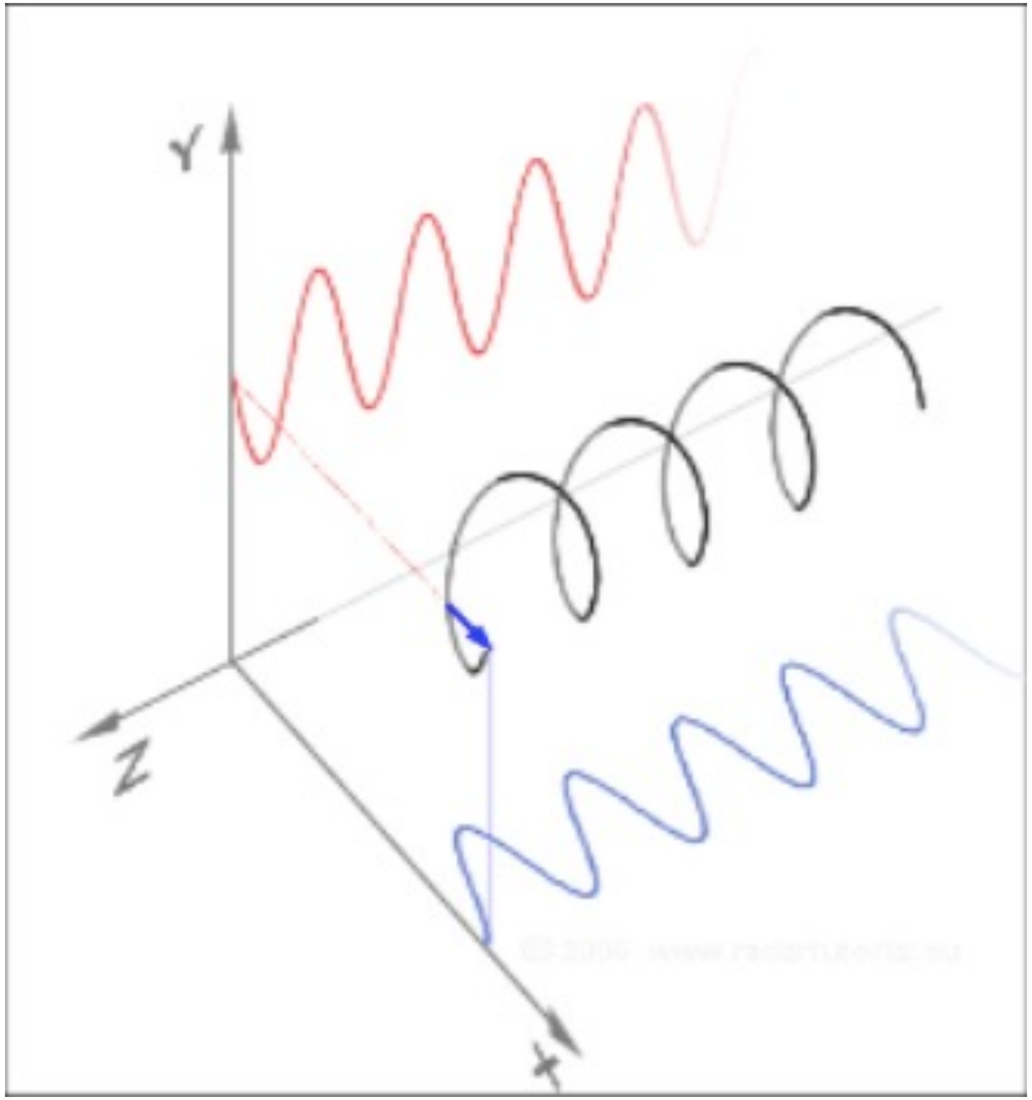

I Total Intensity

Q ↕ − ↔

U ⤡ − ⤢

V ↶ − ↷

Measuring Polarization

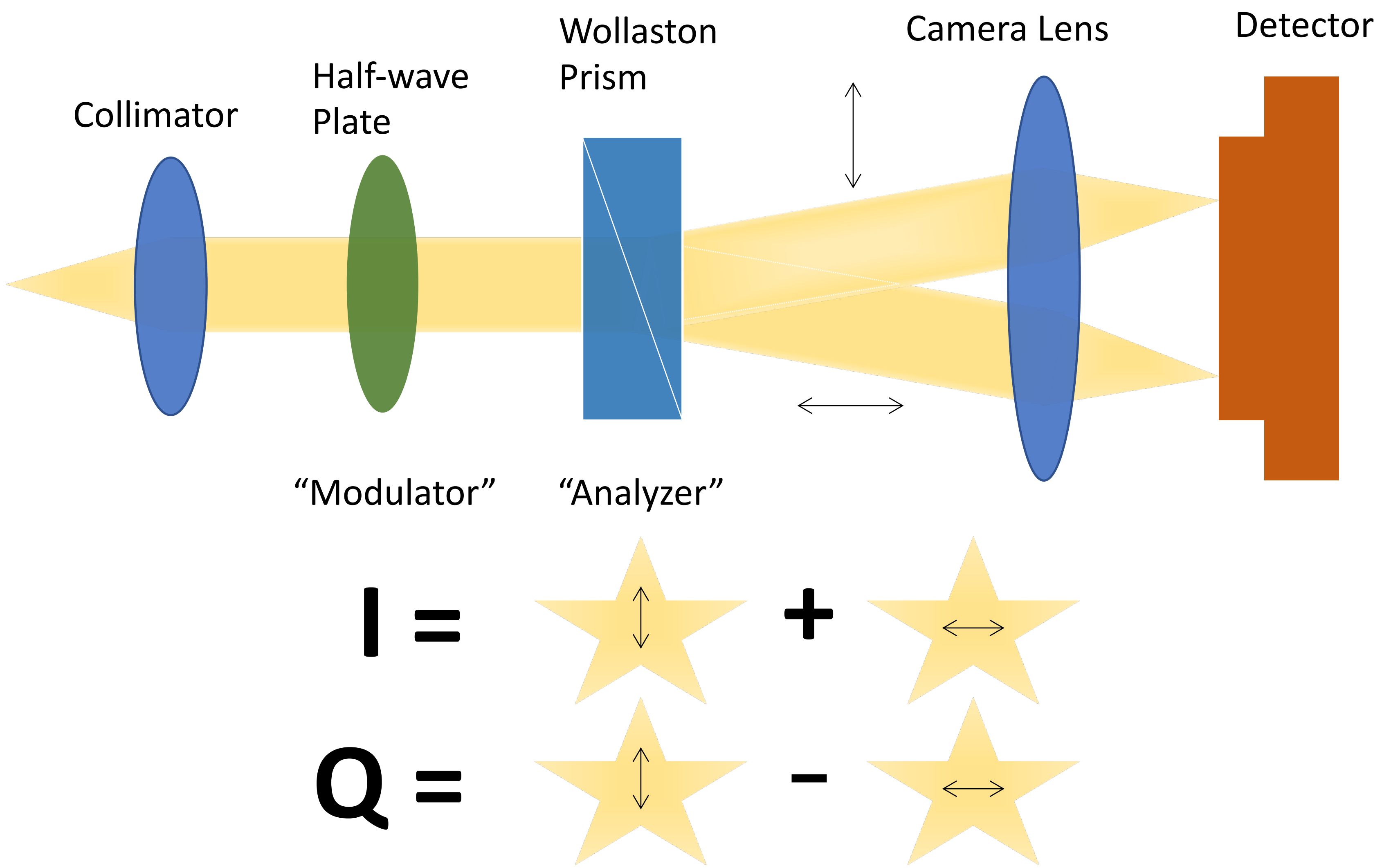

Millar-Blanchaer 2020

Measuring Polarization

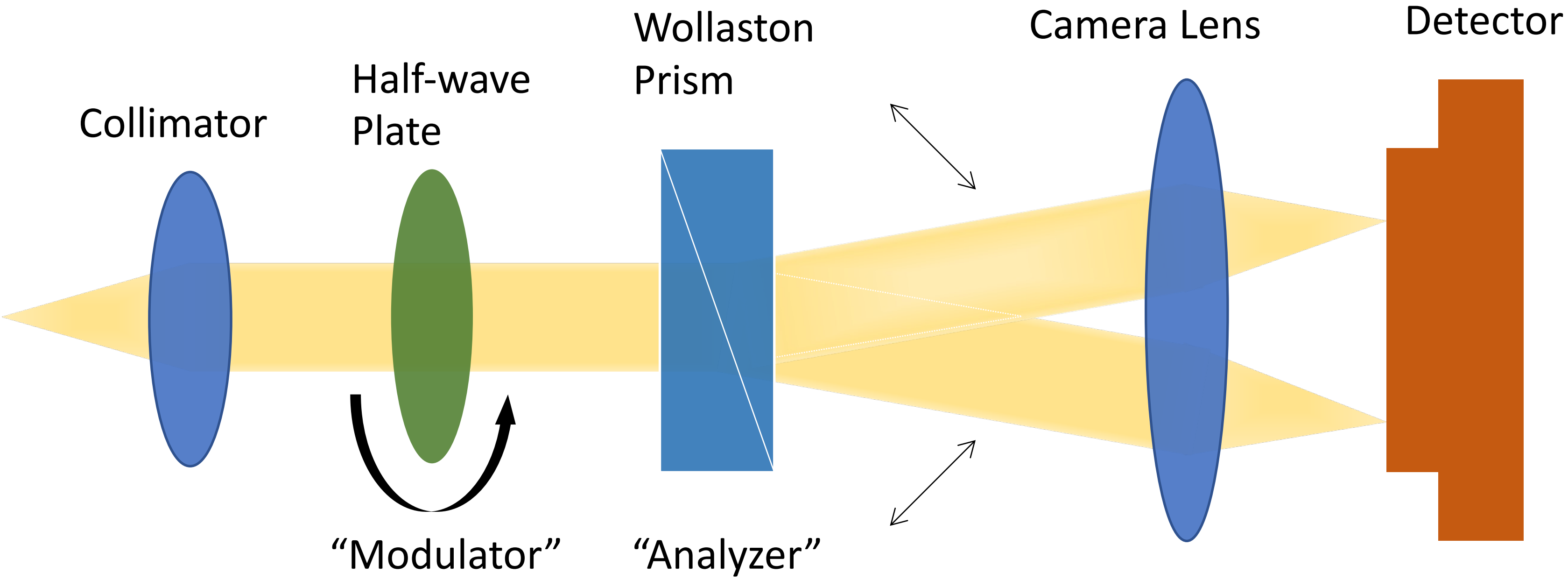

Collimator

Half-wave Plate

“Modulator”

Wollaston Prism

“Analyzer”

Camera Lens

Detector

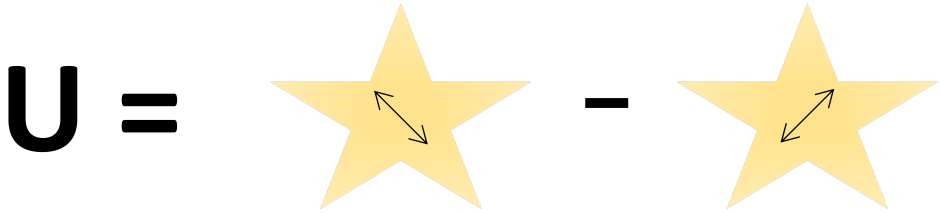

Millar-Blanchaer 2020

Mueller Matrix Representation

$$\begin{pmatrix} I_{\mathrm{in}} \\ Q_{\mathrm{in}} \\ U_{\mathrm{in}} \\ V_{\mathrm{in}} \end{pmatrix}$$

$\mathbf{S}_{\boldsymbol{in}}$

Mueller Matrix Representation

$$\begin{pmatrix} I \rightarrow I & Q \rightarrow I & U \rightarrow I & V \rightarrow I \\ I \rightarrow Q & Q \rightarrow Q & U \rightarrow Q & V \rightarrow Q \\ I \rightarrow U & Q \rightarrow U & U \rightarrow U & V \rightarrow U \\ I \rightarrow V & Q \rightarrow V & U \rightarrow V & V \rightarrow V \end{pmatrix} \begin{pmatrix} I_{\mathrm{in}} \\ Q_{\mathrm{in}} \\ U_{\mathrm{in}} \\ V_{\mathrm{in}} \end{pmatrix}$$

$\boldsymbol{M_{comp}}$ $\boldsymbol{S_{in}}$

Mueller Matrix Representation

$$\begin{pmatrix} \begin{array}{c} I \rightarrow I \\ \boxed{\begin{array}{c} I \rightarrow Q \\ I \rightarrow U \\ I \rightarrow V \end{array}} \end{array} & \begin{array}{c} Q \rightarrow I \\ Q \rightarrow Q \\ Q \rightarrow U \\ Q \rightarrow V \end{array} & \begin{array}{c} U \rightarrow I \\ U \rightarrow Q \\ U \rightarrow U \\ U \rightarrow V \end{array} & \begin{array}{c} V \rightarrow I \\ V \rightarrow Q \\ V \rightarrow U \\ V \rightarrow V \end{array} \end{pmatrix} \begin{pmatrix} I_{\text{in}} \\ Q_{\text{in}} \\ U_{\text{in}} \\ V_{\text{in}} \end{pmatrix}$$

Instrumental
Polarization

$\boldsymbol{M_{comp}}$

$\boldsymbol{S_{in}}$

Mueller Matrix Representation

$$\begin{pmatrix} I \to I & Q \to I & U \to I & V \to I \\ I \to Q & Q \to Q & U \to Q & V \to Q \\ I \to U & Q \to U & U \to U & V \to U \\ I \to V & Q \to V & U \to V & V \to V \end{pmatrix} \begin{pmatrix} I_{\text{in}} \\ Q_{\text{in}} \\ U_{\text{in}} \\ V_{\text{in}} \end{pmatrix}$$

Instrumental Polarization

Crosstalk

$\boldsymbol{M_{comp}}$

$\boldsymbol{S_{in}}$

Mueller Matrix Representation

$$\begin{pmatrix} I_{\text{out}} \\ Q_{\text{out}} \\ U_{\text{out}} \\ V_{\text{out}} \end{pmatrix} = \begin{pmatrix} I \to I & Q \to I & U \to I & V \to I \\ I \to Q & Q \to Q & U \to Q & V \to Q \\ I \to U & Q \to U & U \to U & V \to U \\ I \to V & Q \to V & U \to V & V \to V \end{pmatrix} \begin{pmatrix} I_{\text{in}} \\ Q_{\text{in}} \\ U_{\text{in}} \\ V_{\text{in}} \end{pmatrix}$$

Instrumental Polarization

Crosstalk

$\boldsymbol{S_{out}}$ $\boldsymbol{M_{comp}}$ $\boldsymbol{S_{in}}$

Mueller Matrix Representation

$$M_{retarder} = \begin{pmatrix} 1 & 0 & 0 & 0 \\ 0 & 1 & 0 & 0 \\ 0 & 0 & \cos\phi & sin\phi \\ 0 & 0 & -sin\phi & \cos\phi \end{pmatrix}$$

Mueller Matrix Representation

$$M_{retarder} = \begin{pmatrix} 1 & 0 & 0 & 0 \\ 0 & 1 & 0 & 0 \\ 0 & 0 & \cos\phi & sin\phi \\ 0 & 0 & -sin\phi & \cos\phi \end{pmatrix}$$

$$M_{diattenuator} = \begin{pmatrix} 1 & \varepsilon & 0 & 0 \\ \varepsilon & 1 & 0 & 0 \\ 0 & 0 & \sqrt{1 - \varepsilon^2} & \sqrt{1 - \varepsilon^2} \\ 0 & 0 & -\sqrt{1 - \varepsilon^2} & \sqrt{1 - \varepsilon^2} \end{pmatrix}$$

Mueller Matrix Representation

$$\boldsymbol{S_{out} = M_{Wollaston} \cdot M_{HWP} \cdot S_{in}}$$

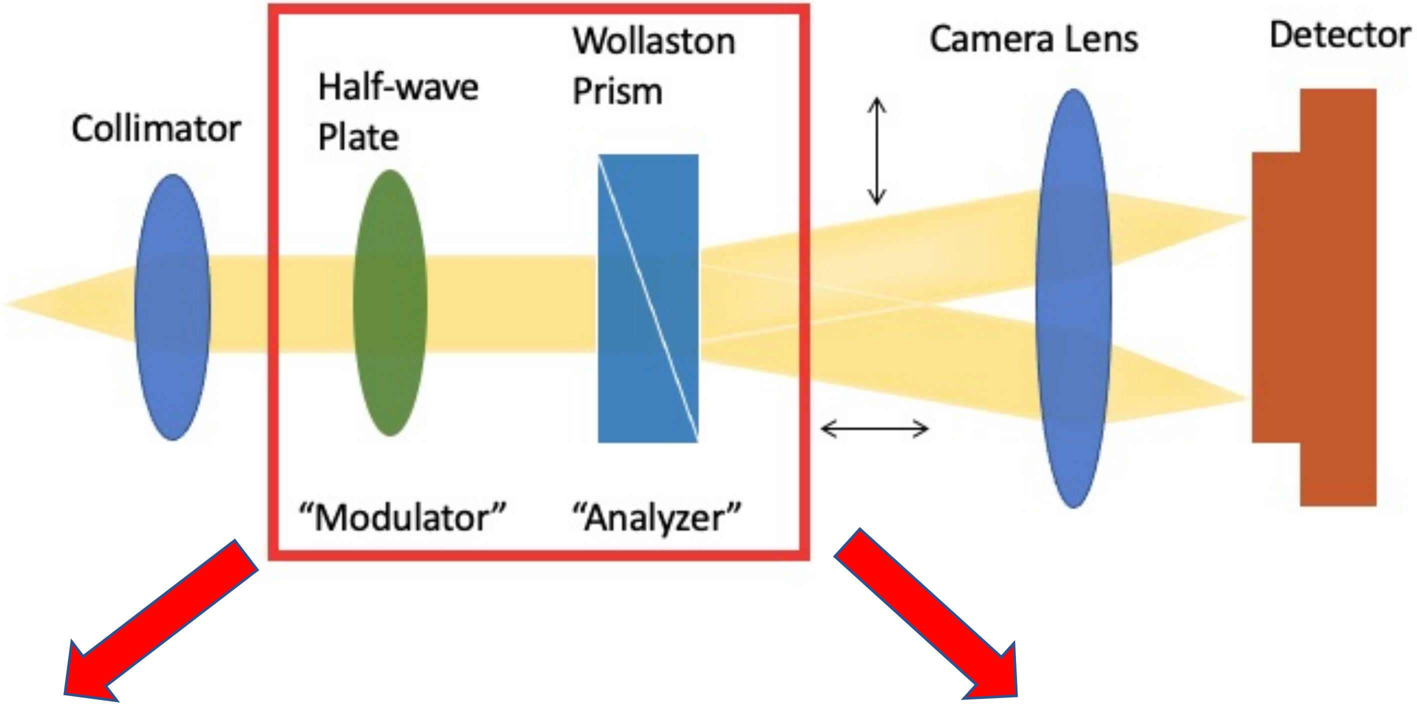

$$M_{HWP} = \begin{pmatrix} 1 & 0 & 0 & 0 \\ 0 & 1 & 0 & 0 \\ 0 & 0 & -1 & 0 \\ 0 & 0 & 0 & 1 \end{pmatrix}$$

$$M_{Wollaston} = \frac{1}{2}\begin{pmatrix} 1 & \pm 1 & 0 & 0 \\ \pm 1 & 1 & 0 & 0 \\ 0 & 0 & 0 & 0 \\ 0 & 0 & 0 & 0 \end{pmatrix}$$

Eleven-Parameter Model

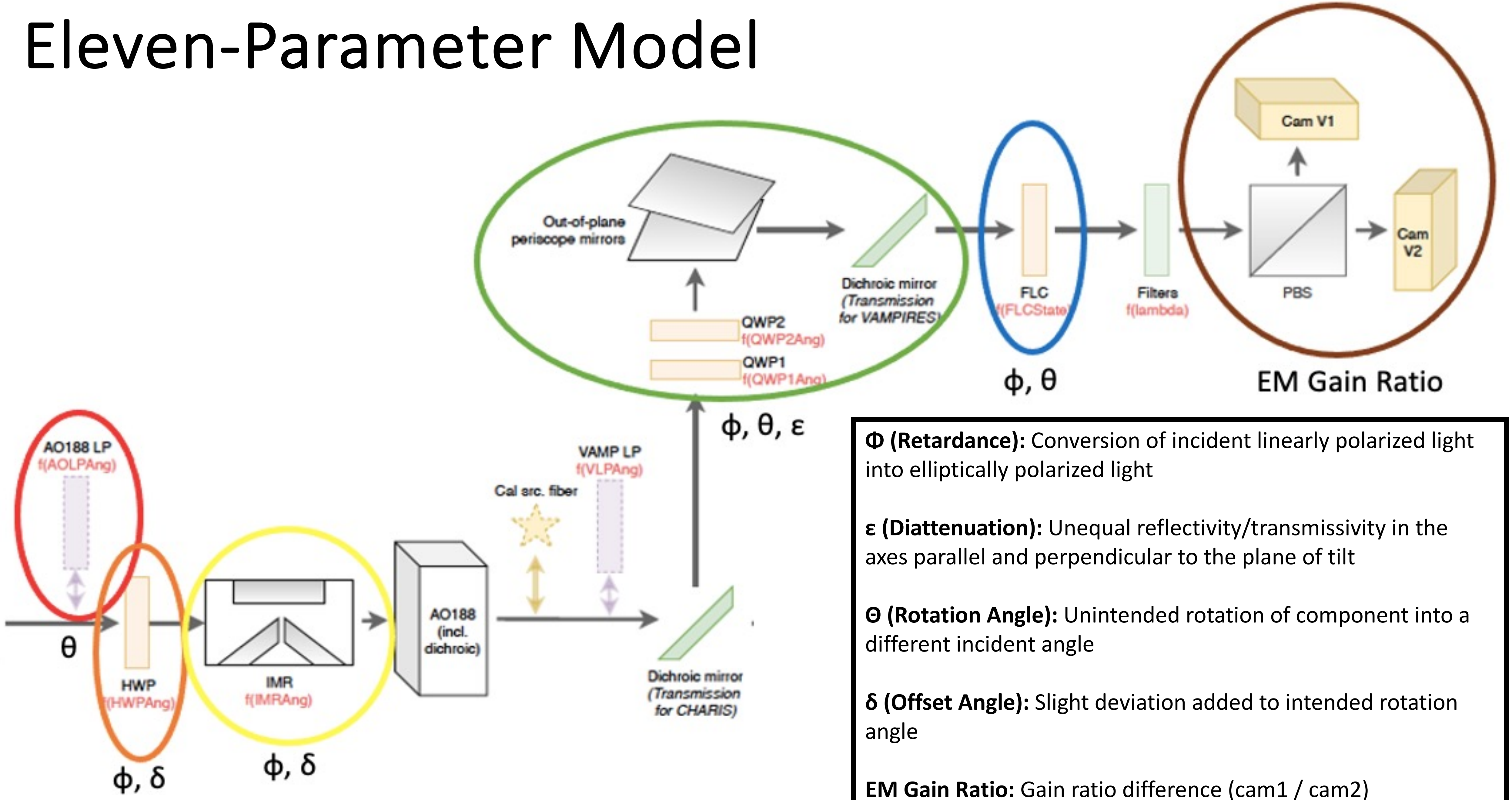

Norris 2021

Φ (Retardance): Conversion of incident linearly polarized light into elliptically polarized light

ε (Diattenuation): Unequal reflectivity/transmissivity in the axes parallel and perpendicular to the plane of tilt

Θ (Rotation Angle): Unintended rotation of component into a different incident angle

δ (Offset Angle): Slight deviation added to intended rotation angle

EM Gain Ratio: Gain ratio difference (cam1 / cam2)

Internal Lab Calibrations: Expressions

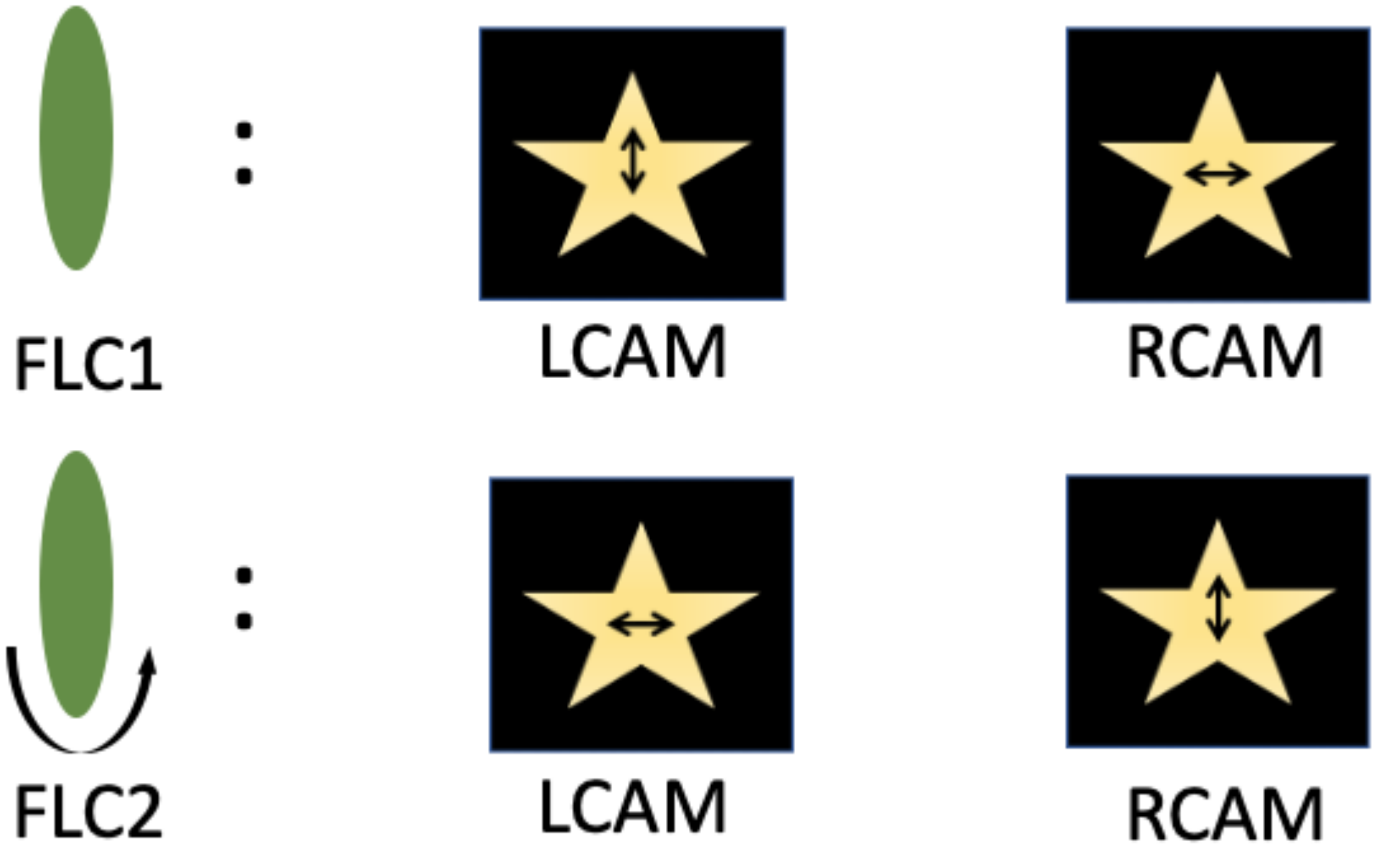

$$D = (L1 - R1) - (L2 - R2)$$

double difference

Internal Lab Calibrations: Expressions

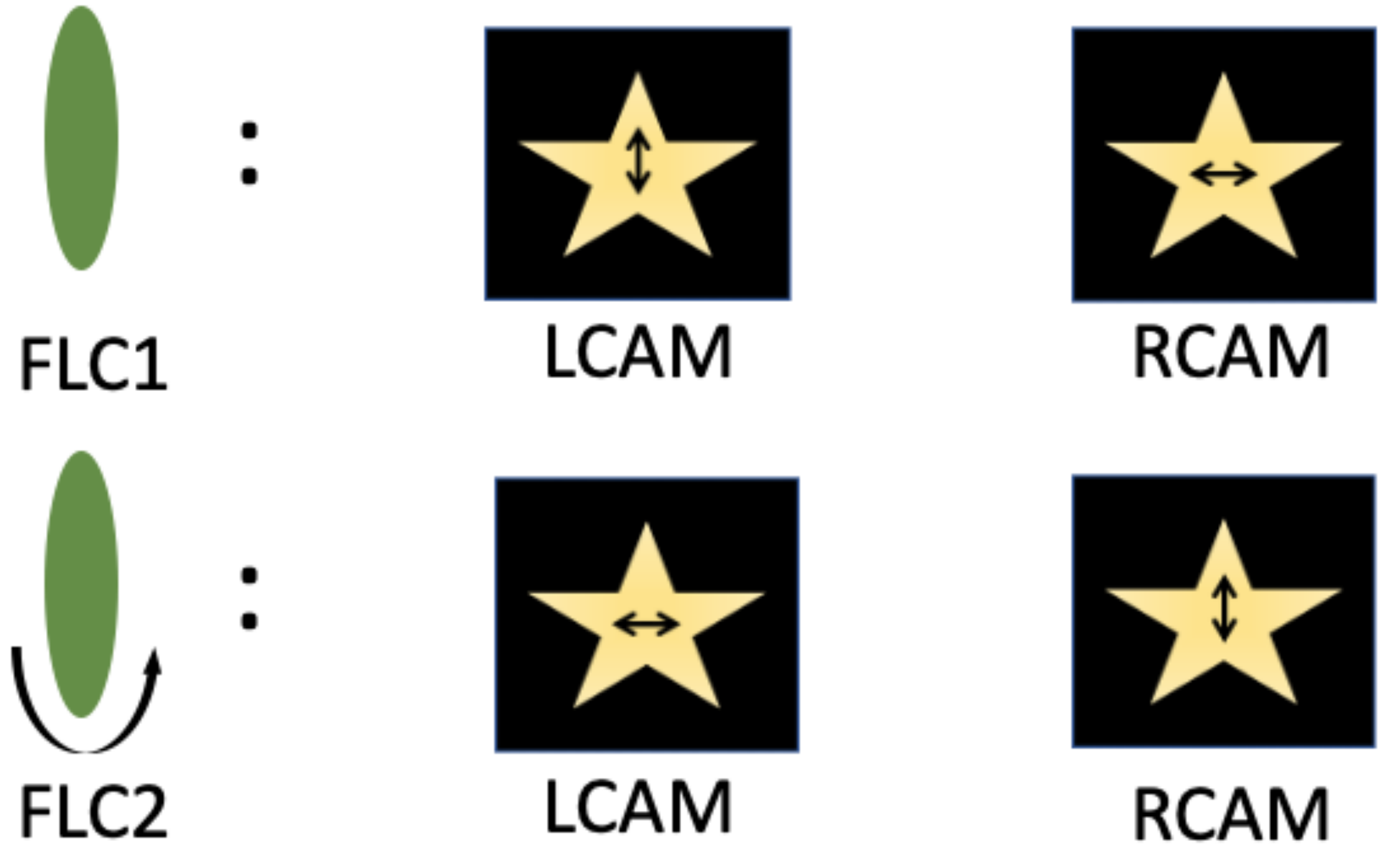

$$S = (L1 - R1) + (L2 - R2)$$

double sum

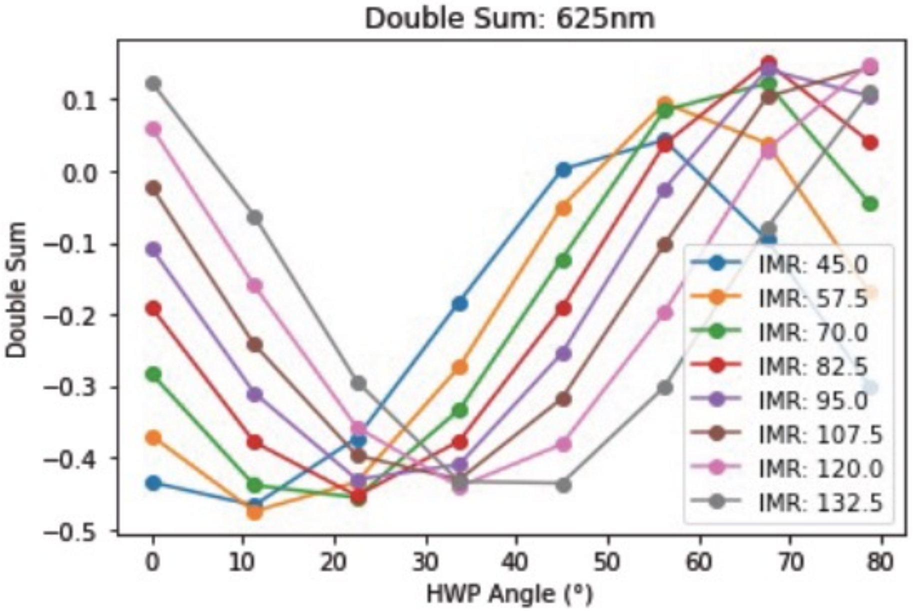
Double Sum: 625nm
Double Sum
HWP Angle (°)
0.1
0.0
−0.1
−0.2
−0.3
−0.4
−0.5
0
10
20
30
40
50
60
70
80
IMR: 45.0
IMR: 57.5
IMR: 70.0
IMR: 82.5
IMR: 95.0
IMR: 107.5
IMR: 120.0
IMR: 132.5

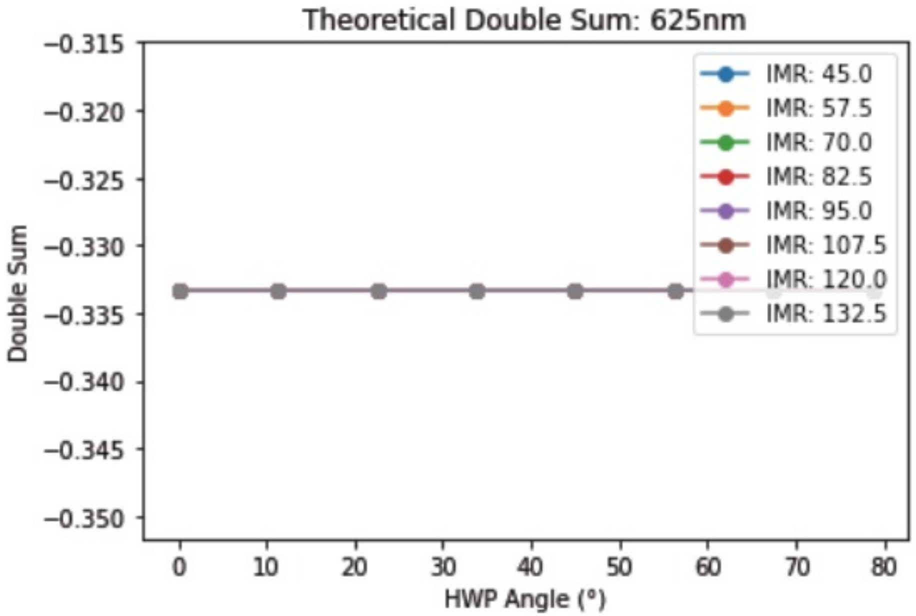
Theoretical Double Sum: 625nm
Double Sum
HWP Angle (°)
−0.315
−0.320
−0.325
−0.330
−0.335
−0.340
−0.345
−0.350
0
10
20
30
40
50
60
70
80
IMR: 45.0
IMR: 57.5
IMR: 70.0
IMR: 82.5
IMR: 95.0
IMR: 107.5
IMR: 120.0
IMR: 132.5

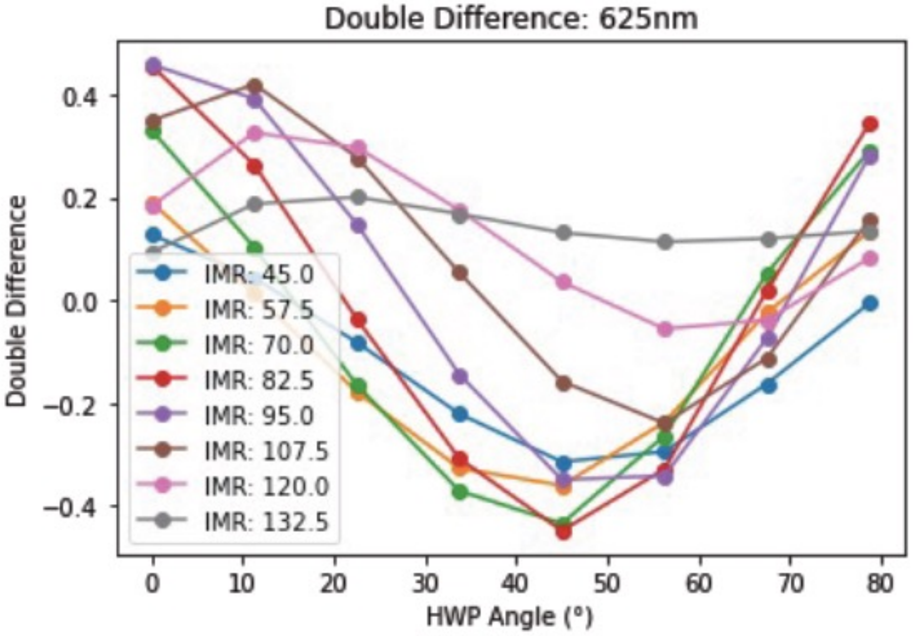
Double Difference: 625nm
Double Difference
HWP Angle (°)
0.4
0.2
0.0
−0.2
−0.4
0
10
20
30
40
50
60
70
80
IMR: 45.0
IMR: 57.5
IMR: 70.0
IMR: 82.5
IMR: 95.0
IMR: 107.5
IMR: 120.0
IMR: 132.5

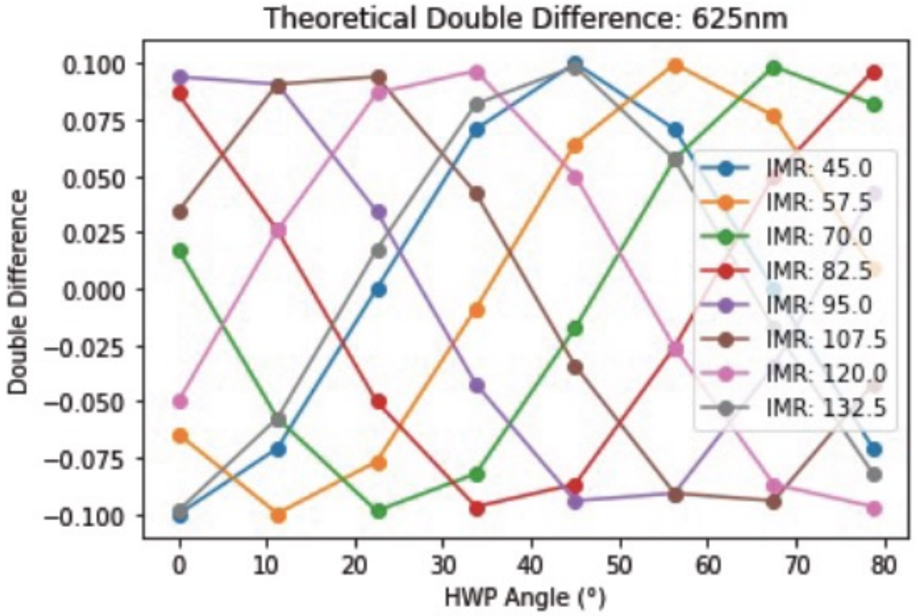
Theoretical Double Difference: 625nm
Double Difference
HWP Angle (°)
0.100
0.075
0.050
0.025
0.000
−0.025
−0.050
−0.075
−0.100
0
10
20
30
40
50
60
70
80
IMR: 45.0
IMR: 57.5
IMR: 70.0
IMR: 82.5
IMR: 95.0
IMR: 107.5
IMR: 120.0
IMR: 132.5

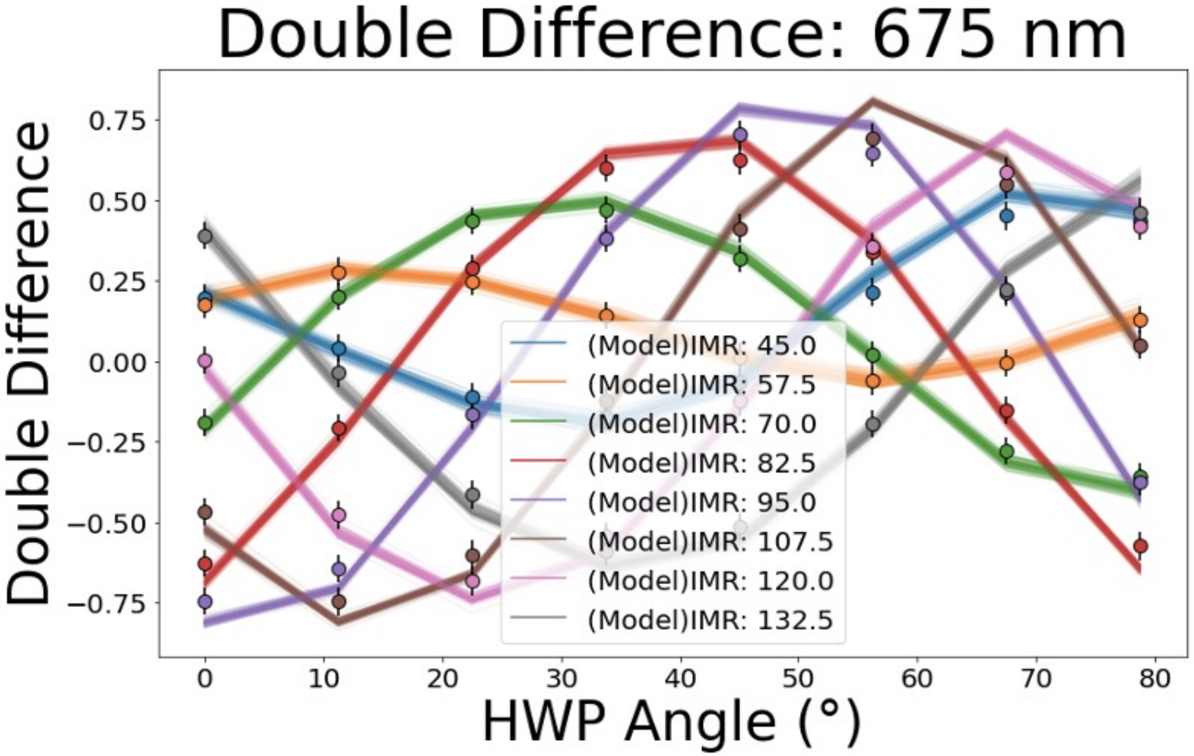
Double Difference: 675 nm
Double Difference
HWP Angle (°)
0.75
0.50
0.25
0.00
−0.25
−0.50
−0.75
0
10
20
30
40
50
60
70
80
(Model)IMR: 45.0
(Model)IMR: 57.5
(Model)IMR: 70.0
(Model)IMR: 82.5
(Model)IMR: 95.0
(Model)IMR: 107.5
(Model)IMR: 120.0
(Model)IMR: 132.5

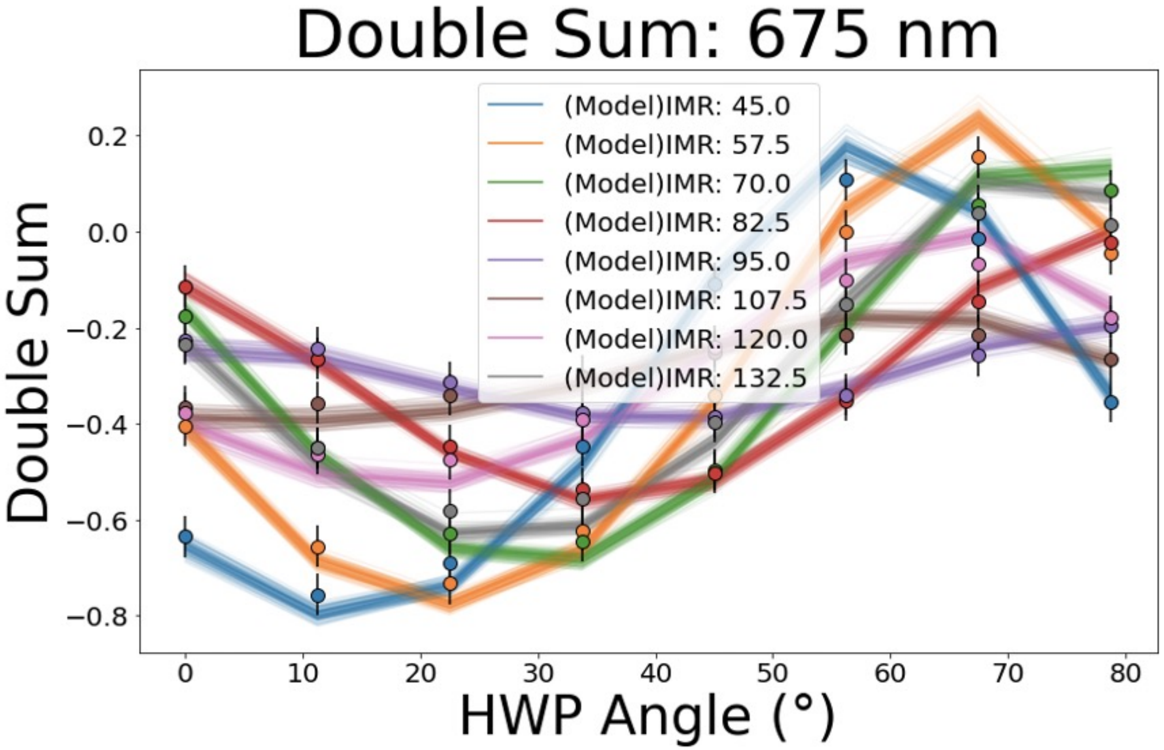
Double Sum: 675 nm
Double Sum
HWP Angle (°)
0.2
0.0
−0.2
−0.4
−0.6
−0.8
0
10
20
30
40
50
60
70
80
(Model)IMR: 45.0
(Model)IMR: 57.5
(Model)IMR: 70.0
(Model)IMR: 82.5
(Model)IMR: 95.0
(Model)IMR: 107.5
(Model)IMR: 120.0
(Model)IMR: 132.5

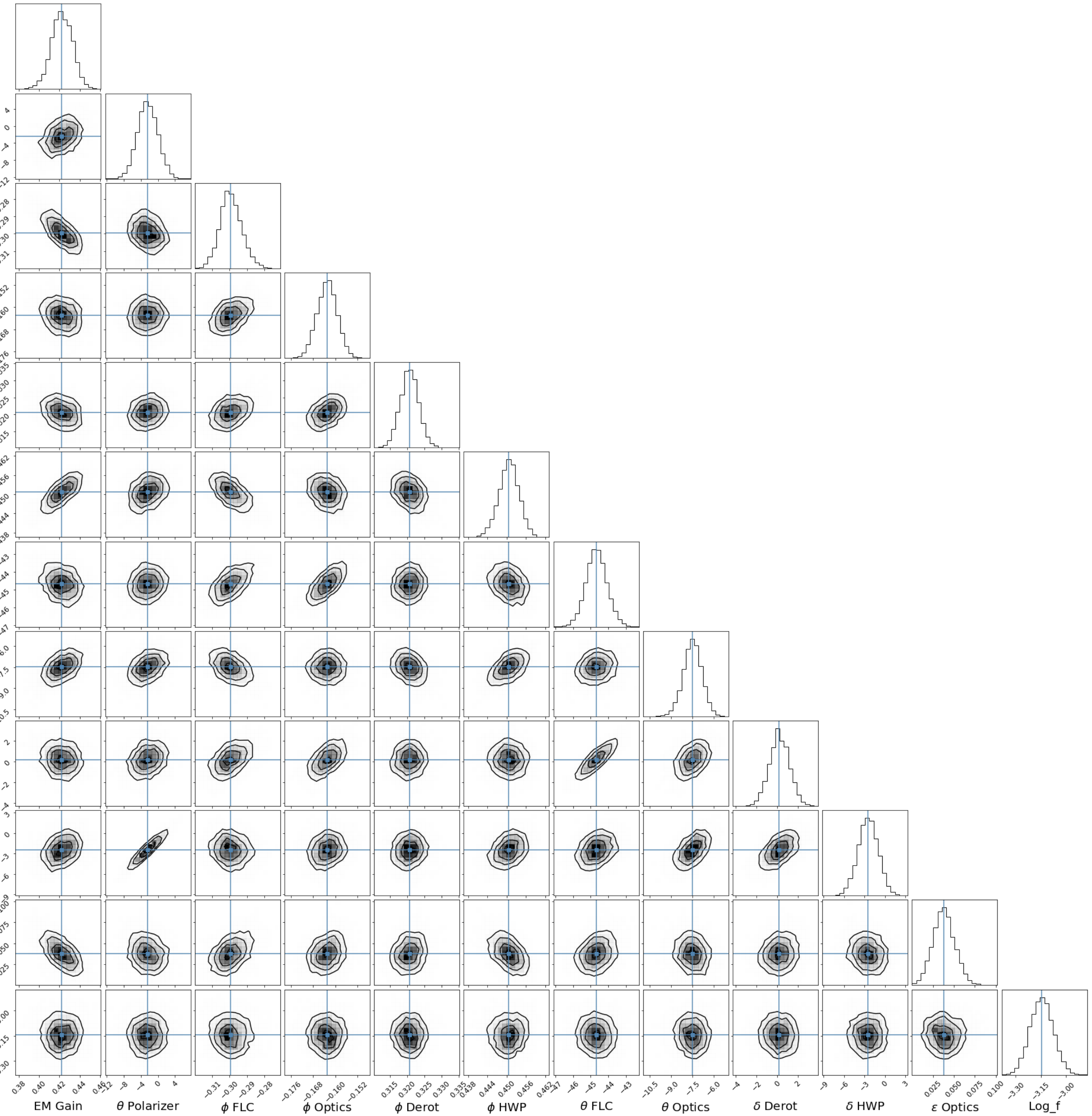
θ Polarizer
φ FLC
φ Optics
φ Derot
φ HWP
θ FLC
θ Optics
δ Derot
δ HWP
ε Optics
Log_f
EM Gain
θ Polarizer
φ FLC
φ Optics
φ Derot
φ HWP
θ FLC
θ Optics
δ Derot
δ HWP
ε Optics
Log_f
0.38 0.40 0.42 0.44 0.46
−12 −8 −4 0 4
−0.31 −0.30 −0.29 −0.28
−0.176 −0.168 −0.160 −0.152
0.315 0.320 0.325 0.330 0.335
0.438 0.444 0.450 0.456 0.462
−47 −46 −45 −44 −43
−10.5 −9.0 −7.5 −6.0
−4 −2 0 2
−9 −6 −3 0 3
0.025 0.050 0.075 0.100
−3.30 −3.15 −3.00

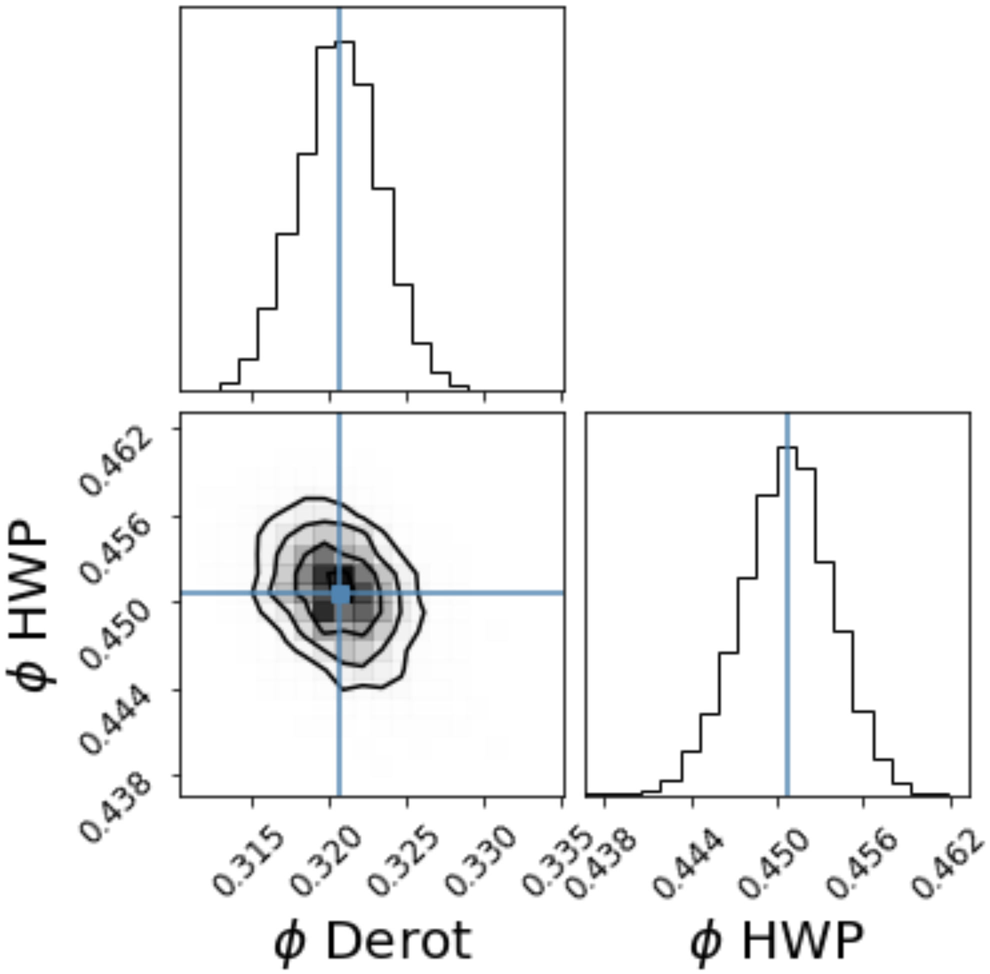

ϕ HWP
0.462
0.456
0.450
0.444
0.438
0.315
0.320
0.325
0.330
0.335
ϕ Derot
0.438
0.444
0.450
0.456
0.462
ϕ HWP

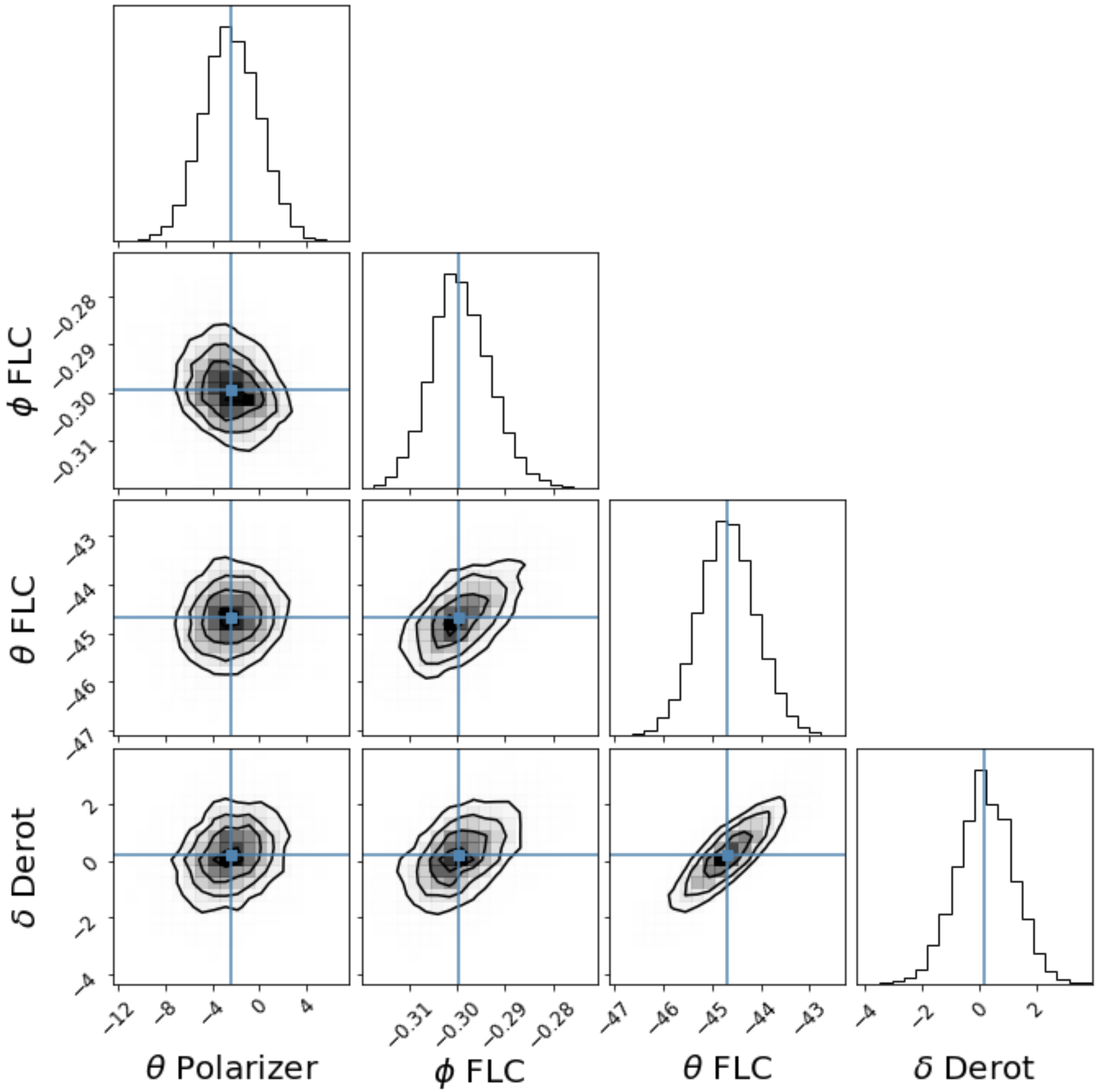

ϕ FLC
-0.28
-0.29
-0.30
-0.31
θ FLC
-43
-44
-45
-46
-47
δ Derot
2
0
-2
-4
-12
-8
-4
0
4
θ Polarizer
-0.31
-0.30
-0.29
-0.28
ϕ FLC
-47
-46
-45
-44
-43
θ FLC
-4
-2
0
2
δ Derot

HWP and IMR Performance

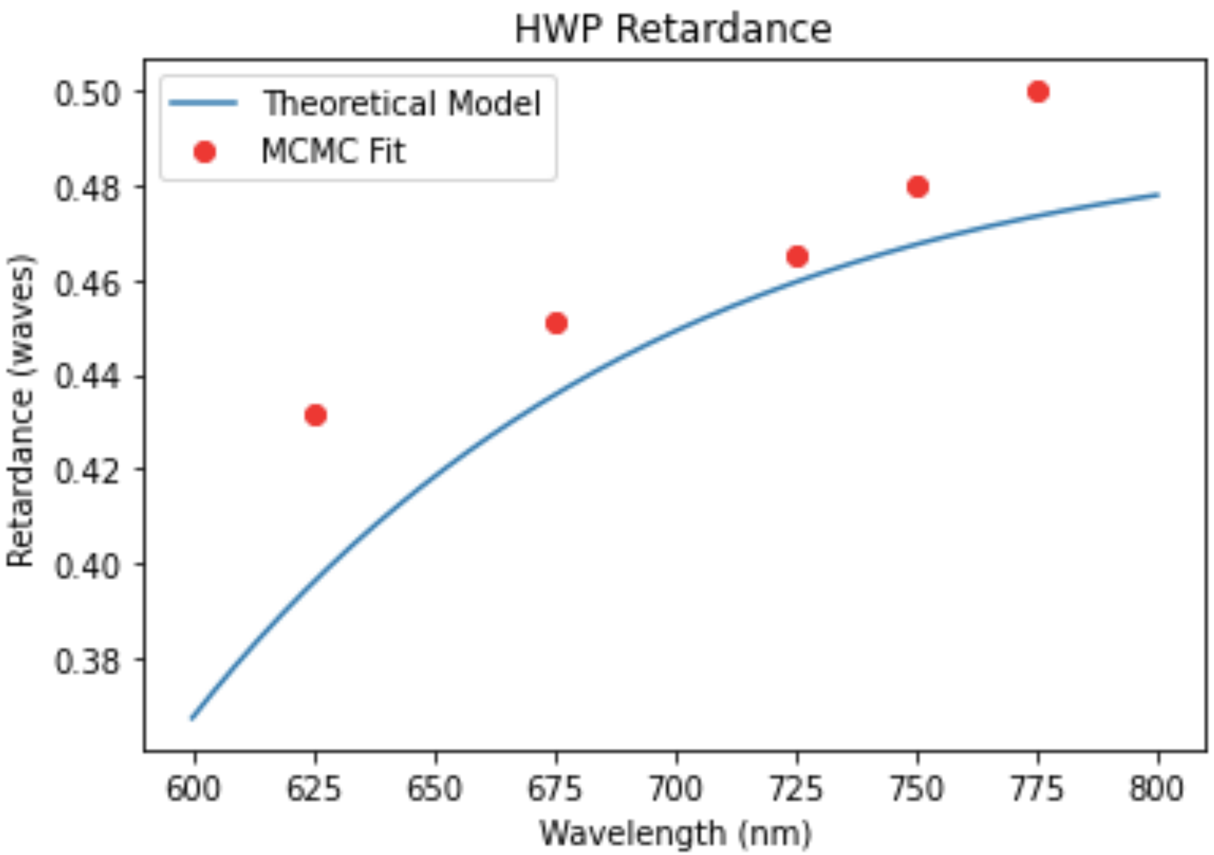

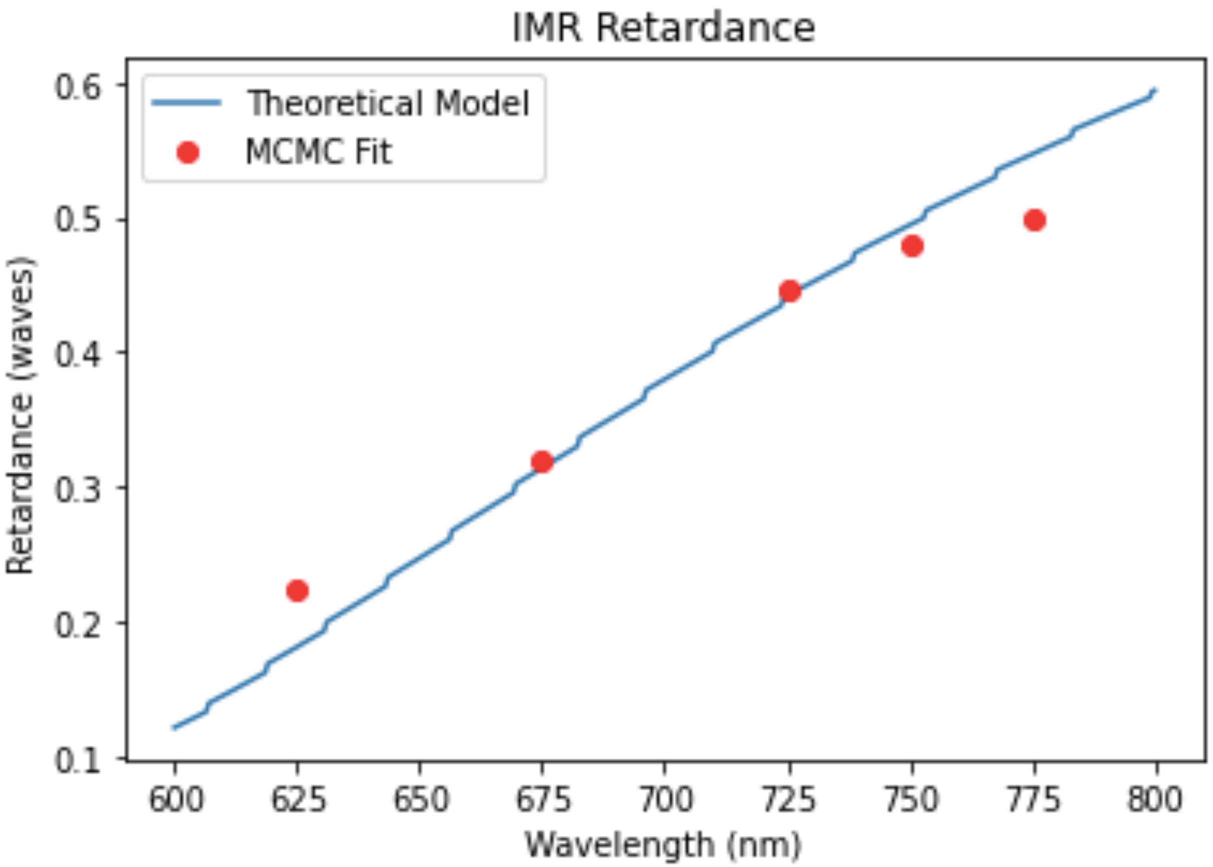

FLC Performance

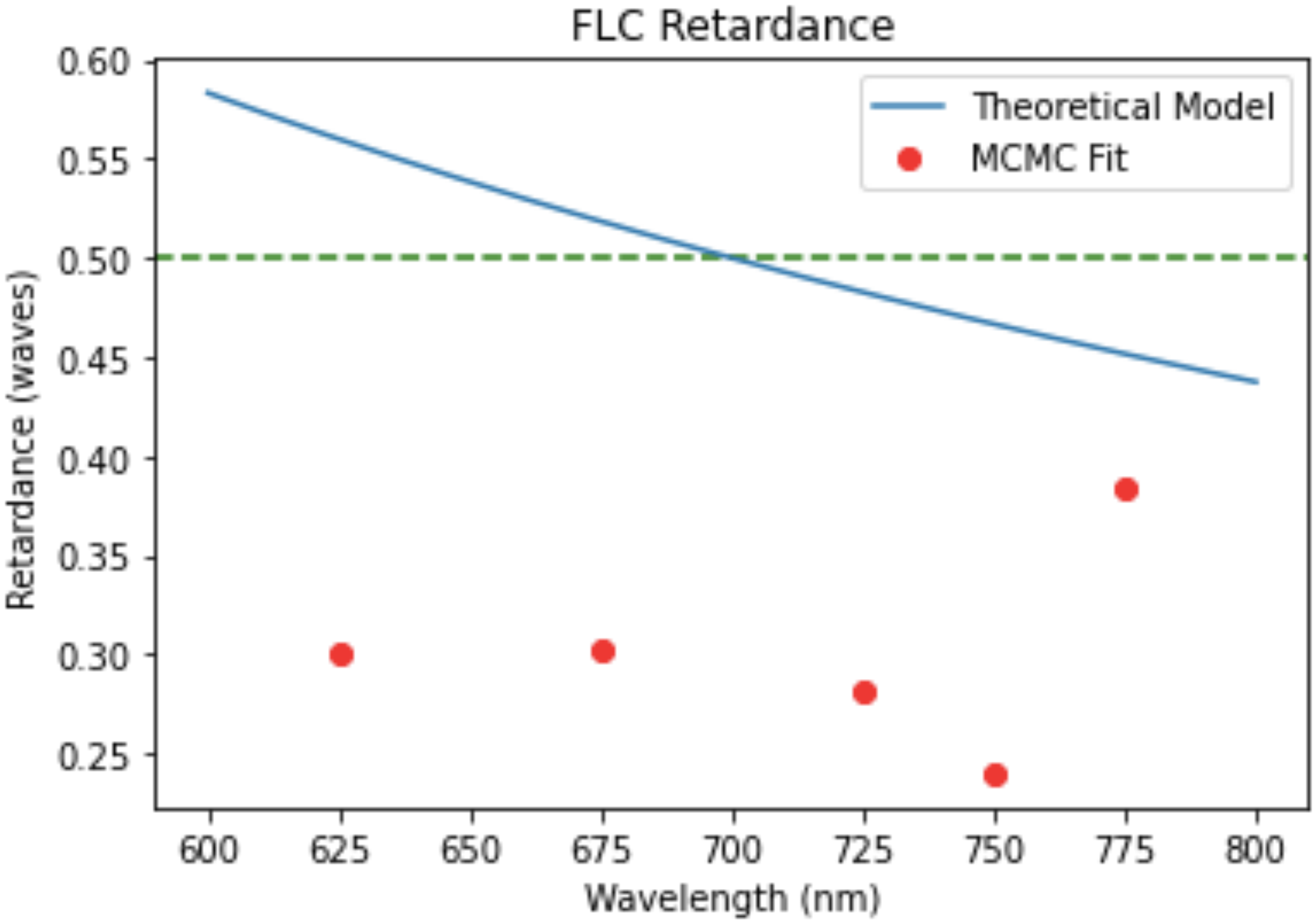

Lucas 2023

HD34700

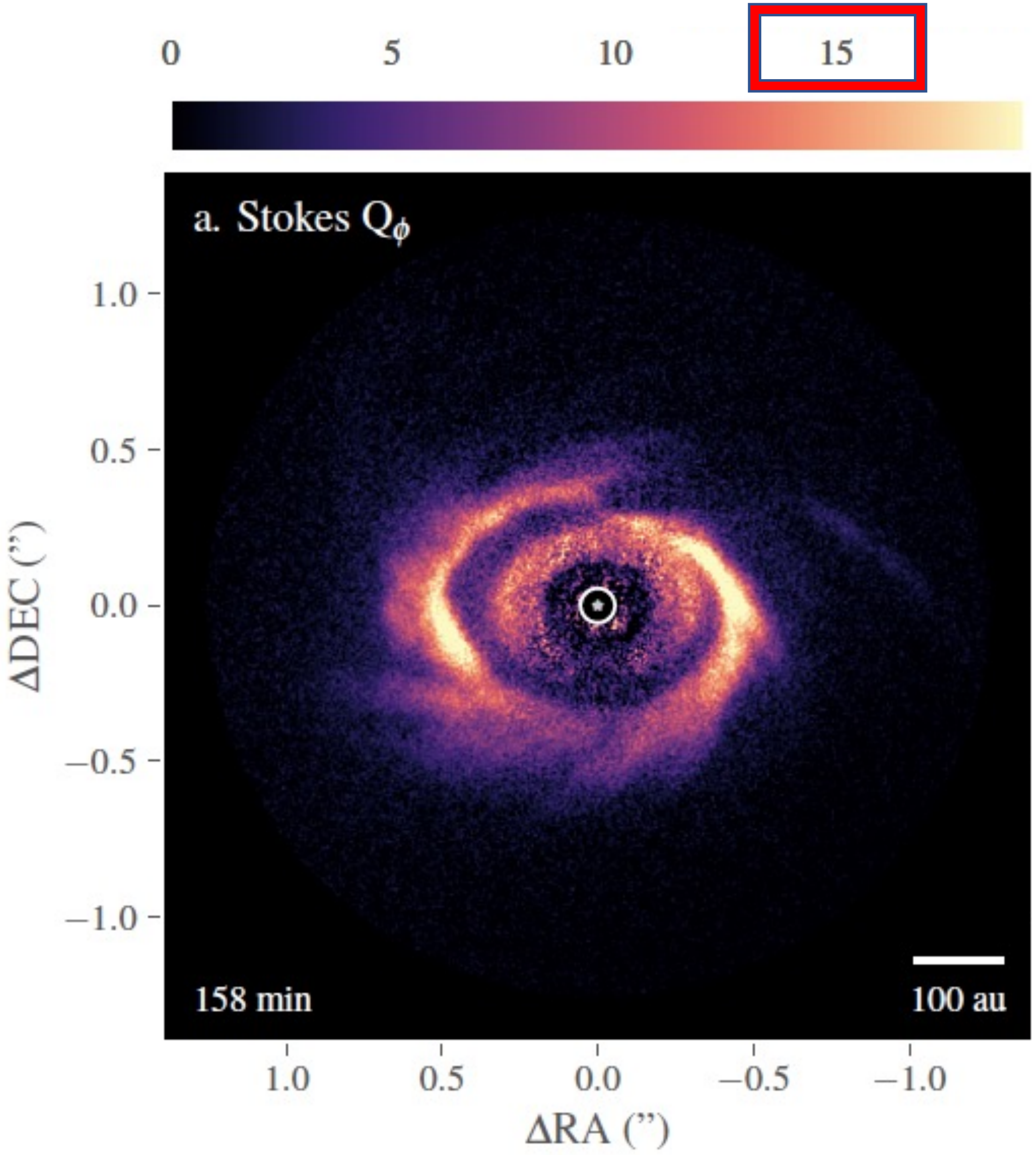

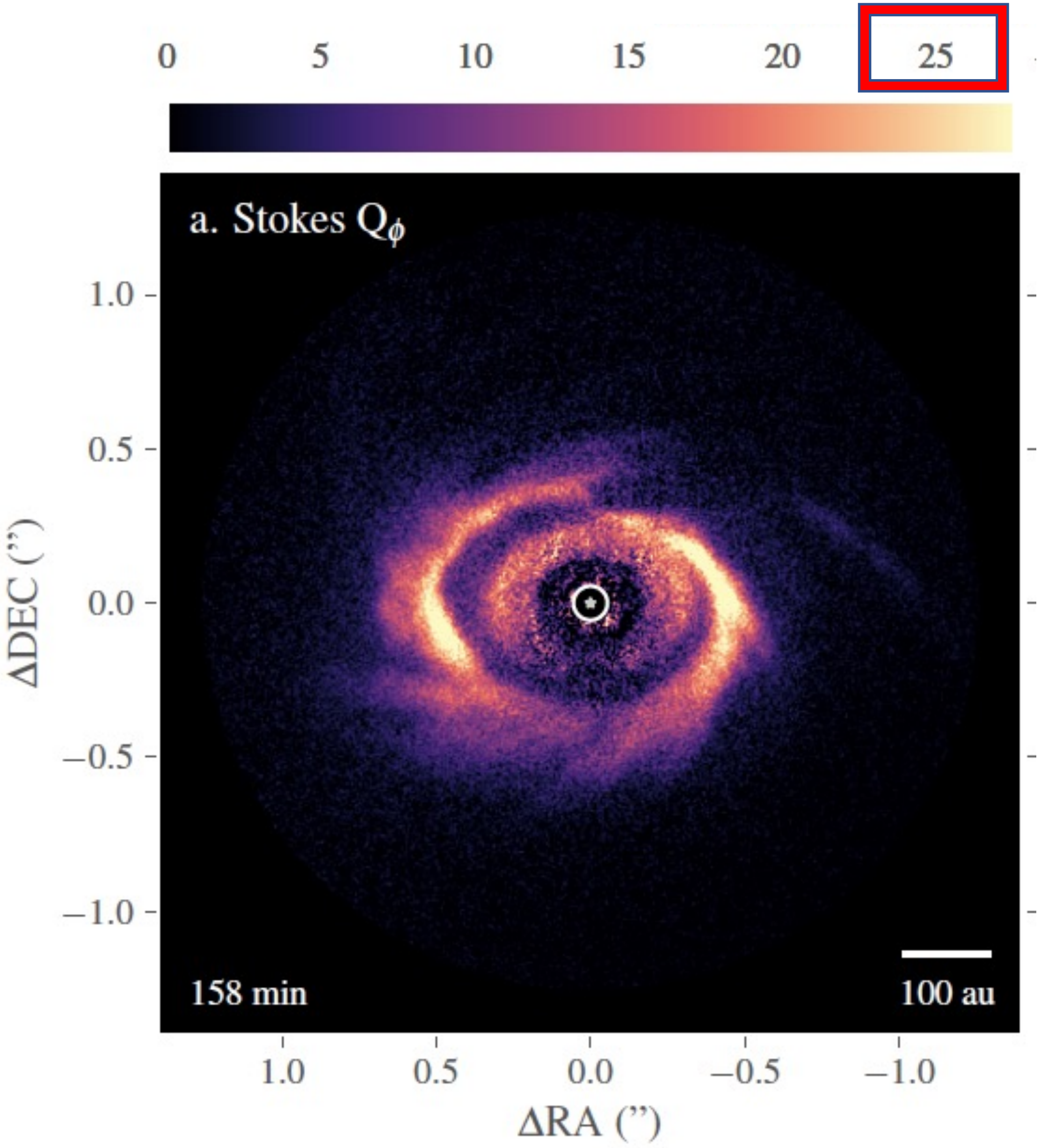

Internal Lab Calibrations: Takeaways

- Highly non-ideal and wavelength-dependent behaviour
- Confirmation of HWP and IMR retardance physical models
- Confirmation of anomalous behaviour at 625 and 775 nm
- Many sources of degeneracy
- FLC retardance deviates significantly from 1/2 wave
- Camera EM gain drift

Conclusions

- Retroactive parameter extraction is time-consuming
  - Isolated calibrations for each component is invaluable
- Regular lab and on-sky calibrations are needed to track IP changes

Next Steps

- Determination of diattenuation and retardance of M3
- Verification of polarized standards
- Developing a calibration routine
- Apply on more science data!

VAMPIRES 2023 Upgrade

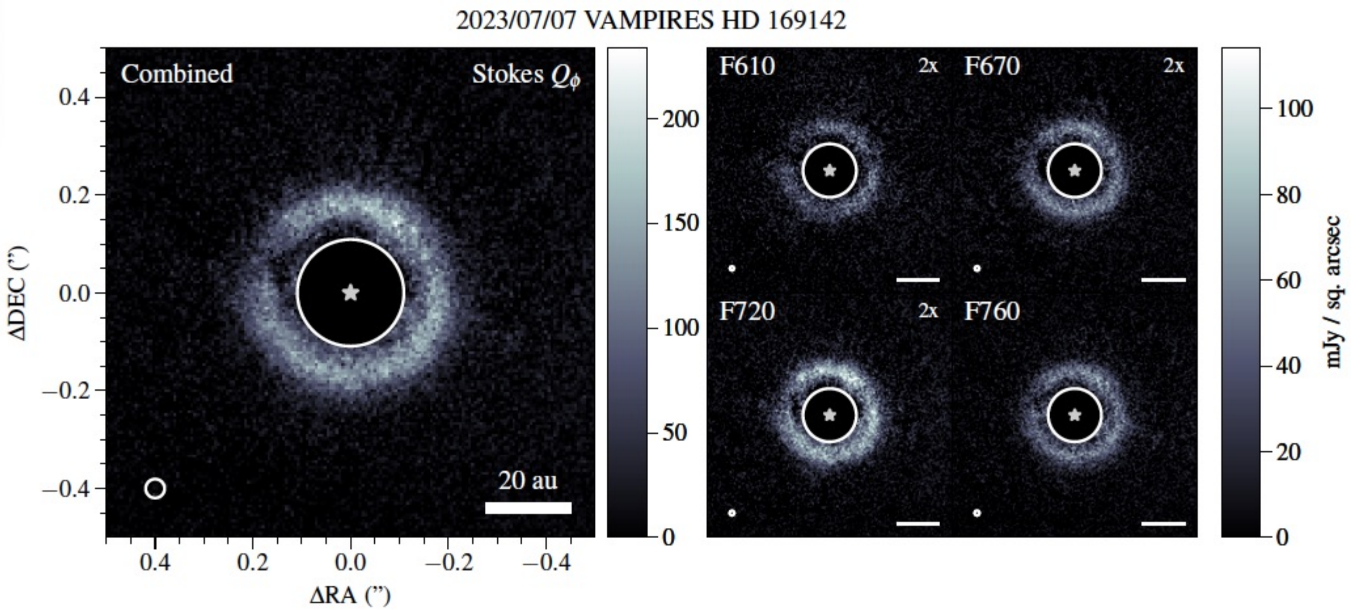

Lucas 2023

- New multiband imaging mode
- New achromatic FLC
- Some of the highest dynamic range of any SCExAO instruments